

# Morphology as Algorithm: Deriving Reward Prediction Error from the Physics of Dendritic Geometry

Weicheng Tang Yonghui Niu

Nanjing University

{231880309, 231880317}@smail.nju.edu.cn

## Abstract

Brains lack dedicated subtraction circuits for  $\delta = R - V$ , yet error learning is foundational. We propose **neuronal geometry as RPE hardware code**. Using an active dendrite model, we show RPE is physically enforced by Ohm’s law between soma (prediction) and distal dendrites (reality). Axial voltage gradients encode “surprise” and “disappointment” into currents driving Hebbian updates. This analog mechanism, requiring no digital circuits, enables emergent “epiphany” and “risk-aversion.” Code: <https://github.com/bailan137/neuron>.

## 1 Introduction

Silicon uses ALUs for subtraction; biological “wetware” RPE ( $\delta = R - V$ ) faces physical constraints. We propose a first-principle approach: **Morphology transforms “subtraction” into “gradient equilibrium.”** The neuron acts as a physical comparator: (1) **Soma** integrates history, its membrane potential representing the **Prediction (V)**; (2) **Dendrites** receive environmental inputs, their local depolarization representing the **Reward/Reality (R)**; (3) **Morphology** connects them via **Axial Resistance ( $R_a$ )**. When  $R \neq V$ , potential differences generate axial currents representing physical RPE, driving learning.

## 2 Related Work

Since London [7], views on dendritic computation shifted from perceptrons [4] to morphology.

**1. Single Neurons as DNNs:** Cortical neurons match 5-8 layer DNNs [2]. Masoli et al. [8] attribute this to morphological complexity. We ground RPE in this structure.

**2. Dendritic Logic:** Branches are functional units [3]. Beyond XOR [5] and binding [11], we prove morphology performs analog “subtraction.”

**3. Isolation & Feedback:** Subtraction needs isolation and feedback. Compartmentalization provides isolation [1]; bAPs provide feedback [10]. Combining stochastic growth [9], our model uses  $R_a$  and bAPs to physically reproduce dual-mechanism coding [6].

## 3 Methods and Model Construction

We use the NEURON simulation environment to build a multi-compartment model that accurately captures spatiotemporal ion dynamics.

**1. Morphology:** We adopt a classic “Ball-and-Stick” topology.

- **Soma:** A sphere with both diameter and length of  $20\mu m$ , serving as the integration hub for the “prediction” signal ( $V$ ).
- **Dendrite:** A  $500\mu m$  long,  $2\mu m$  diameter cylinder, divided into 51 segments (‘nseg=51’) for fine-grained simulation.
- **Core Parameters:** Axial resistance  $R_a$  is set to  $150\Omega \cdot cm$  and membrane capacitance  $c_m$  to  $1\mu F/cm^2$  for all sections.

The long dendrite with high axial resistance is key to “Ohmic subtraction,” decoupling distal reality ( $R$ ) from proximal prediction ( $V$ ) to create meaningful voltage gradients.

**2. Ion Channel Gradients:** We implement heterogeneous Hodgkin-Huxley (HH) type channel densities.

- **Soma:** High density of fast  $Na^+$  ( $\bar{g}_{Na,hh} = 0.3 S/cm^2$ ) and  $K^+$  ( $\bar{g}_{K,hh} = 0.036 S/cm^2$ ) channels to ensure reliable action potential (AP) generation.
- **Dendrite:** A moderate  $Na^+$  channel density ( $\bar{g}_{Na,hh} = 0.052 S/cm^2$ ) supports back-propagating APs (bAPs) but not initiation. High-threshold  $Ca^{2+}$  channels ( $\bar{g}_{Ca,HVA} = 0.01 S/cm^2$ ) and a calcium pump (‘cad’) with a decay time of  $\tau_{cad} = 50ms$  are located distally ( $> 250\mu m$  from soma).
- **Synapses:**
- **Excitatory:** NMDA-like synapses (‘Exp2Syn’) with  $\tau_{rise} = 1ms$ ,  $\tau_{decay} = 30ms$ , and  $E_{rev} = 0mV$ . Spatially distributed synapses incorporate intrinsic conduction delays from 0 to  $12ms$ .
- **Inhibitory (Risk):** A GABAa-like synapse at the proximal dendrite (‘dend(0.1)’) with  $E_{rev} = -80mV$  produces powerful shunting inhibition.

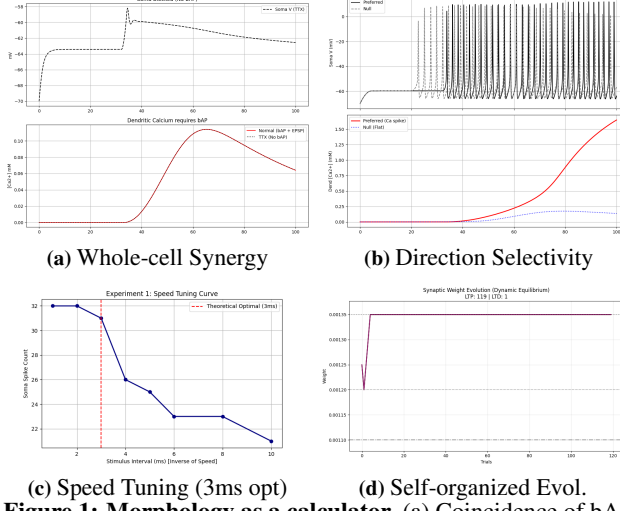


**Figure 1: Morphology as a calculator.** (a) Coincidence of bAP and EPSP triggers a dendritic calcium plateau. (b) This enables direction selection. (c) The structure resonates with specific input timings. (d) It guides weights to a stable representation.

## 4 Experiments and Analysis

### 4.1 Phase 1: Geometric Perception

Dendritic geometry shapes how the neuron filters spatiotemporal patterns.

(1) **Coincidence Detection.** A dendritic calcium plateau emerges only when a somatic bAP meets a distal EPSP (Fig. 1a). Silencing somatic  $\text{Na}^+$  channels removes the plateau, confirming its bAP dependence. This interaction directly produces direction selectivity (Fig. 1b).

(2) **Speed Tuning.** Acting as a physical delay line, the dendrite shows a resonance peak when inputs arrive  $\sim 3\text{ms}$  apart, revealing a preferred stimulus speed (Fig. 1c).

(3) **Self-Organization.** A calcium-threshold plasticity rule (LTP if  $[\text{Ca}^{2+}]_{\text{peak}} > 0.107 \mu\text{M}$ ; LTD otherwise) drives synapses toward a stable pattern under mixed-direction stimulation (Fig. 1d).

### 4.2 Phase 2: Physical Derivation of RPE

We compute RPE by directly reading out the axial voltage gradient. In the model, the agent’s confidence sets a somatic clamp  $V_{\text{soma}}$ , while feedback (`is_correct`) controls distal synaptic drive.

$$I_{\text{axial}} = \frac{V_{\text{dend}} - V_{\text{soma}}}{R_{\text{axial}}} \propto \text{RPE} \quad (1)$$

Fig. 2a shows a clean mapping between voltage gradients and behavioral outcomes:

**Surprise ( $R > V$ ).** Low confidence paired with reward produces a positive gradient ( $V_{\text{dend}} > V_{\text{soma}}$ ), generating inward current that supports LTP.

**Disappointment ( $R < V$ ).** High confidence without reward reverses the gradient, producing outward current consistent with LTD. In effect, the neuron implements RPE through

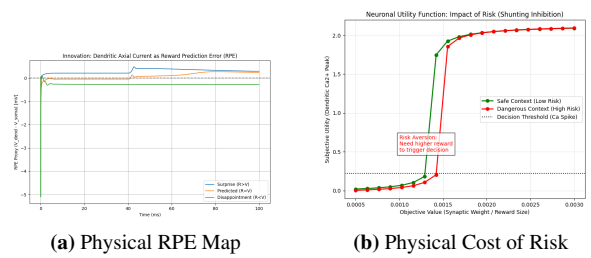


**Figure 2: Physical mechanisms of learning and choice.** (a) A positive voltage gradient (Surprise, blue) drives inward current for LTP; a negative gradient (Disappointment, green) drives outward current for LTD. (b) Proximal shunting inhibition leaks current, increasing the threshold for action, physically encoding risk aversion.

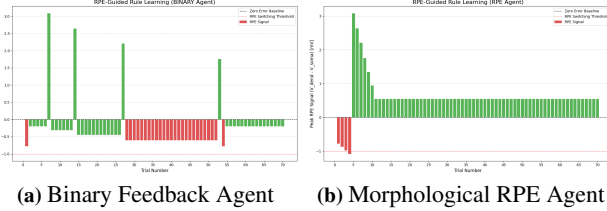


**Figure 3: The Epiphany Moment.** (a) A binary agent oscillates, struggling to find the correct rule. (b) The morphological agent experiences a large, continuous RPE signal, leading to a decisive, one-shot “epiphany” and stable learning.

a simple Ohmic voltage difference—turning subtraction into physics.

### 4.3 Phase 3: Emergent Behavior: Epiphany & Risk Aversion

**1. Epiphany vs. Oscillation:** We compared two learning agents in a cognitive loop. A control agent using binary “correct/incorrect” feedback oscillates when faced with a difficult rule (Fig. 3a). In contrast, our agent uses the **continuous, signed, analog RPE signal** from the neuron. A massive negative RPE signal (e.g.,  $-1.0\text{mV}$ ), representing an “extreme surprise,” physically forces a decisive, one-shot switch in the agent’s hypothesis. This emerges as an “Epiphany” moment in the learning curve (Fig. 3b), a behavior impossible with simple digital feedback.

**2. The Physics of Risk Aversion:** Modeling risk as proximal shunting inhibition ( $g_{\text{inh}}$ ) shifts the neuron’s input-output curve to the right (Fig. 2b). Physically, the inhibitory conductance acts as a “leak” in the dendritic cable, shunting excitatory currents away before they reach the soma. Consequently, a much stronger synaptic input (a higher “reward”) is required to overcome this leak and reach the decision threshold (e.g.,  $\text{Ca}^{2+}$  spike). **1**Risk aversion is not an abstract calculation but the direct physical energy cost required to overcome shunting inhibition.

## 5 Conclusion

Our simulations identify neuronal geometry as the hardware for reinforcement learning: (1) Dendrites are spatiotemporal filters, (2) Axial resistance is a physical subtractor, and (3)

Voltage gradients are the error signal. Intelligence arises from structure; geometry downscale high-level "subtraction" to low-level physical "flow," offering a blueprint for novel, physics-based computing architectures.

## References

- [1] L. Beaulieu-Laroche, E. H. Toloza, M.-S. Van der Goes, M. Lafourcade, D. Barnagian, Z. M. Williams, E. N. Eskandar, M. P. Frosch, S. S. Cash, and M. T. Harnett. Enhanced dendritic compartmentalization in human cortical neurons. *Cell*, 175(3):643–651, 2018.
- [2] D. Beniaguev, I. Segev, and M. London. Single cortical neurons as deep artificial neural networks. *Neuron*, 109(17):2727–2739, 2021.
- [3] T. Branco and M. Häusser. The single dendritic branch as a fundamental functional unit in the nervous system. *Current opinion in neurobiology*, 20(4):494–502, 2010.
- [4] N. Brunel, V. Hakim, P. Isopé, J.-P. Nadal, and B. Barbour. Optimal information storage and the distribution of synaptic weights: perceptron versus purkinje cell. *Neuron*, 43(5):745–757, 2004.
- [5] A. Gidon, T. A. Zolnik, P. Fidzinski, F. Bolduan, A. Papoutsis, P. Poirazi, M. Holtkamp, I. Vida, and M. E. Larkum. Dendritic action potentials and computation in human layer 2/3 cortical neurons. *Science*, 367(6473):83–87, 2020.
- [6] H. S. Kim, G. M. Santana, G. Sancer, T. Emonet, and J. M. Jeanne. Divergent synaptic dynamics originate parallel pathways for computation and behavior in an olfactory circuit. *Current Biology*, 2025.
- [7] M. London and M. Häusser. Dendritic computation. *Annu. Rev. Neurosci.*, 28(1):503–532, 2005.
- [8] S. Masoli, D. Sanchez-Ponce, N. Vrieler, K. Abu-Haya, V. Lerner, T. Shahar, H. Nedeaescu, M. F. Rizza, R. Benavides-Piccione, J. DeFelipe, et al. Human purkinje cells outperform mouse purkinje cells in dendritic complexity and computational capacity. *Communications Biology*, 7(1):5, 2024.
- [9] X. Ouyang, S. Sutradhar, O. Trottier, S. Shree, Q. Yu, Y. Tu, and J. Howard. Neurons exploit stochastic growth to rapidly and economically build dense dendritic arbors. *Nature Communications*, 16(1):5903, 2025.
- [10] G. Stuart and M. Häusser. Initiation and spread of sodium action potentials in cerebellar purkinje cells. *Neuron*, 13(3):703–712, 1994.
- [11] Y. Tang, S. Jia, T. Huang, Z. Yu, and J. K. Liu. Implementing feature binding through dendritic networks of a single neuron. *Neural Networks*, page 107555, 2025.

## A Author Contributions

**Yonghui Niu** Conceptualization, initial model implementation, manuscript revision and supervision. 50% contribution.

**Weicheng Tang** Initial manuscript draft, experimental design and execution, code organization and finalization. 50% contribution.